14IND10 MET5G A1.1.1

Literature review of wireless link quality metrics

Project Number: JRP 14IND10

Project Title: Metrology for 5G Communications (MET5G)

Document Type: Activity Report

Authors: Tian Hong Loh (NPL)
Martin Hudlička (CMI)
Tim Brown (University of Surrey)
Zhengrong Tian (NPL)
David A. Humphreys (NPL)

Contents

Executive summary

The objective of this review was to perform a literature review that collated, defined and critically reviewed the most important metrics used to assess wireless link quality. This involved consultation with industry directly and through industry groups and standards bodies to understand the industry needs. Variety of definitions of the signal-to-interference-plus-noise ratio (SINR) have been identified for different scenarios, starting from existing 3G/4G solutions to the future prospective systems, such as MIMO, device to device and millimeter-wave frequencies considerations. Extensive patent search has been performed and the most influential works related to interference evaluation have been summarized. This document also discusses scenarios categories within which the SINR is calculated differently and different variables in each case.

The SINR, in its basic form, is expressed as a ratio of signal to the sum of interference signals plus Gaussian white noise. However, dependent on the scenario, it can also bring about a dependency on time, distance, polarisation, angular pattern and frequency. All scenarios are bandwidth dependent. In terms of 5G technology requirements it is necessary to quantify defined scenarios where interference has an impact on quality of service, both to the new 5G system but also in terms of legacy services using neighbouring spectrum bands.

List of abbreviations

Abbreviation	Description
A-HARQ	Adaptive Hybrid Automatic Repeat Request
AWGN	Additive White Gaussian Noise
BER	Bit Error Rate
CCDF	Complimentary Cumulative Distribution Function
CCI	Co-Channel Interference
CDMA	Code Division Multiple Access
CSI	Channel State Information
CQI	Channel Quality Indicator
eNB	evolved-Node B, term for a base station in 4G systems
E-UTRA	Evolved Universal Terrestrial Radio Access
FEC	Forward Error Correction
HSDPA	High-Speed Downlink Packet Access
ICI	Inter-Channel Interference
IN	Impulsive Noise
ISI	Inter-Symbol Interference
LTE	Long-Term Evolution
MAC	Medium Access Control
MCS	Mobile Switching Centre
MIMO	Miltiple-Input Multiple-Output
OFDM	Orthogonal Frequency Division Multiplexing
OFDMA	Orthogonal Frequency Division Multiple Access
PDF	Probability Distribution Function
PDR	Packet Delivery Ratio
RSRP	Reference Signal Receive Power
RSRQ	Reference Signal Receive Quality
RSS	Received Signal Strenght
RSSI	Received Signal Strength Indicator
SINR	Signal-to-Interference-plus-Noise Ratio
SISO	Single-Input Single-Output
SMV	Squared Mean by Variance
SNR	Signal-to-Noise Ratio
UE	User Equipment, term for a mobile terminal in 4G systems
UWB	Ultra-Wide Band
WGN	White Gaussian Noise

1 Introduction

1.1 Overview

The objective was to perform a literature review that collated, defined and critically reviewed the most important metrics used to assess wireless link quality. This involved consultation with industry directly and through industry groups and standards bodies to understand the industry needs.

The signal-to-interference-plus-noise ratio (SINR) is a quantity which is widely used in theoretical studies of channel capacity in wireless communications [1]. In this context interference is deemed to be any unwanted signal that is picked-up from other communications system, or between components within a system. In the event that there are no interfering sources, the quantity SINR reduces to the signal-to-noise ratio (SNR), which has been the main quantity of interest in wired communications systems. The complexity of contemporary wireless communication networks in a real radio environment causes the SNR to vary among different users by tens of decibels. In a wireless system with many concurrent transmissions, signal-to-interference-plus-noise ratio (SINR) becomes a relevant figure of merit of the system.

1.2 Material covered

There are many coding schemes that are currently in operation so in order to provide a definition that is not biased towards a particular communications system and that will be useful for the development of 5G we have considered several different modulation formats. Also, we have investigated the patent literature as this tends to focus on commercial application. 5G embodies a number of extended or new features such as massive MIMO and direct (device to device) communication. Also 5G plans to use millimeter-wave frequencies that have previously normally been used only in fixed or satellite environments. There will be an emphasis on the later generation of systems because these are likely to be closer to the 5G structure.

1.3 UE SINR measurement

Fig. 1 illustrates a generic wireless communication system. The estimation of SINR is typically undertaken at the output of the demodulator and input of the decoder. If the SINR has a dependence on the channel model used then this must be recorded as part of the test conditions.

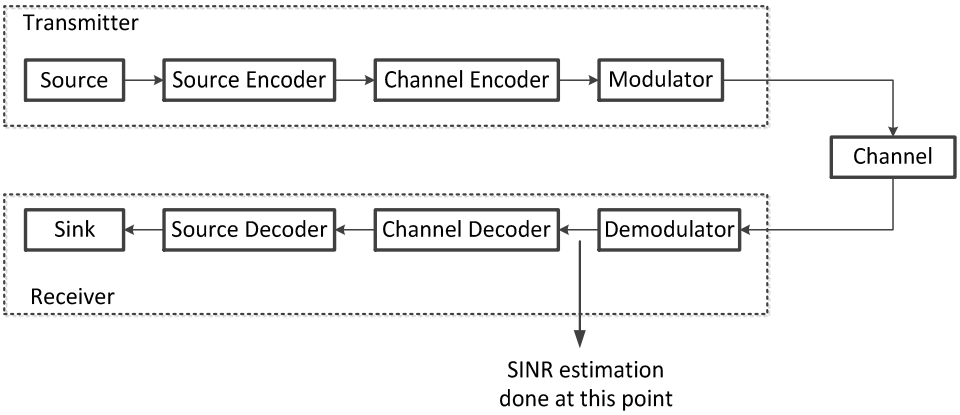

Figure 1: Generic wireless communication system.

SINR can be defined at different levels. The first level, also the fundamental level, is the *instantaneous SINR* per resource element (RE), which is the ratio between the useful signal amplitude and the level of interference and noise (see Fig. 2). Typically, the useful signal amplitude is estimated through a pilot-aided channel estimator. A signal regeneration (SR) estimator is used to obtain the interference and noise level by subtracting the useful symbols from the received symbols.

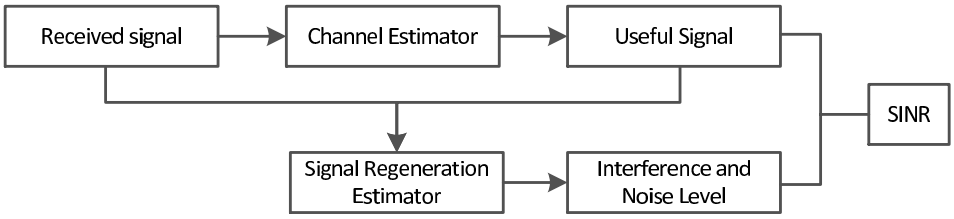

Figure 2: Instantaneous SINR measurement.

The above process can be done for each resource element to obtain SINR per resource element. Multiple SINR per RE within a resource block (RB) is combined to form *effective SINR* per RB, through a suitable compression function (see Fig. 3). The most famous forms of effective SINR include the exponential effective SINR, the geometric mean effective SINR, and the mutual information exponential effective SINR. The effective SINR is then mapped to a scalar CQI and reported to eNodeB.

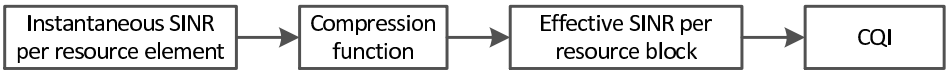

Figure 3: Effective SINR measurement.

SINR is defined and internally measured by most UE vendors on Resource Block basis. UE computes SINR for each RB and converts it to CQI and report to eNodeB for MCS selection, power control and etc. For different application, different SINR may be desirable:

For power control and fast rate adaption, such as HSDPA, it is desirable to track the short-term fading as much as possible. In this situation, instantaneous SINR is useful. For certain applications such as handoff decisions and slow rate adaption (e.g. GSM, GPRS), *average SINR* is alternatively defined using average over several adjacent time slots. Accurate SINR estimation provides a more efficient system and a higher user-perceived quality of service. However, UE chipset and RF scanner manufacturers implement SINR measurement in various different ways which are not always easily comparable. Various SINR measurement patents reflect the facts that currently SINR is being measured by different ways tackling different aspect of SINR problems.

2 Pre-existing material

2.1 Interference models

2.1.1 Ultrawideband communications

Performance of UWB communications in the presence of interference is outlined in [2]. Although UWB is not directly related to 5G communications, the paper contains valuable definitions and comparison to carrier-based communications and interference issues. Since gigahertz unoccupied slices of bandwidth are not available at microwave frequencies, under FCC regulations UWB radio must be treated as spurious interference to all other communication systems. The paper deals with analyzing jam resistance properties of UWB systems and comparing them to those of direct-sequence spread-spectrum (DS-SS). Jam resistance with rectangular pulses and with monocycles (Gaussian and Rayleigh) is analyzed. The same interference with a certain bandwidth W_j could be narrowband with respect to UWB and wideband with respect to direct-sequence spread spectrum. For UWB, the parameter α was defined as pulse-width times interference bandwidth. This definition can be extended to DS-SS, where the pulsewidth is the chip time T_c. For DS-SS, $\alpha = T_c W_j$. Thus, α serves as a measure of comparative bandwidth between the interference and either system. The mechanisms for interference suppression are quite different for both the UWB and DS-SS. With DS-SS, the interference is typically spread by cross-correlation with the PN sequence and is subsequently reduced by lowpass filtering at the data bandwidth. In contrast with UWB there are two mechanisms for interference suppression: 1) time windowing over the duration of

the short UWB pulse and 2) the cross correlation at the receiver of the interference with the template $V(t) = p(t) - p(t-\delta)$ results in reduction of a narrowband interference due to the high correlation of the interference at times t and $t \pm T_p$ ($p(t)$ is time-domain representation of the monocycle). It was shown that for both narrowband and wideband interference, UWB has a significant advantage in interference suppression ability over DS-SS.

Authors of [3] derived an analytical expression for average SINR for UWB Rake receiver in an indoor multiuser communication scenario, given that the interference level is fluctuating due to asynchronous transmission among different users. The indoor wireless channel model adopted was a standard channel model released by IEEE 802.15 study group 3a. In this model, the multipath components arrive according to a double Poisson process and the fading coefficient of each multipath component has an independent log-normal distribution rather than Rayleigh distribution. Based on the derived framework, the performance of UWB Rake receiving system in different types of indoor wireless channels can be compared, using the analytical SINR as a performance measure.

2.1.2 3G/4G wireless channel interference

The noise in current communications systems can be divided into two parts: white Gaussian noise (WGN) and impulsive noise (IN). To characterize WGN, it is sufficient to know the root mean square (RMS) noise level. However, the IN component is much more difficult to characterize since the parameters that describe IN cannot be measured directly. Instead, these parameters are later determined in the data processing. The measurement equipment has to collect samples at a very high speed to obtain the following IN parameters [4]: number of bursts, burst level or amplitude, burst length or duration, burst separation. There has been an effort to harmonize the impulsive noise measurement methods (frequency selection, measurement time, detector etc., see [5]).

A comprehensive review of radio wave propagation in an industrial environment is presented in [6]. The wireless channel in an industrial environment behaves very differently compared with the radio channels in home and office environments. This is due to the presence of significant noise and interference effects caused by large machinery and heavy multipath propagation effects caused by highly reflective structures. The article [6] compares measured path-loss parameters of many types of industrial environment. The bursty behaviour of the IN is modelled by a two-state first-order Markov process $n(t) = w(t) + b(t)\,k(t)$ for $t \in \{1,\ 2,\ \ldots,\ T\}$, where $w(t)$ and $k(t)$ are Gaussian distributed processes with zero-means. Parameter $n(t)$ describes the AWG noise plus impulse noise. When the channel is in a good state, i.e., $b(t) = 0 \ \rightarrow \ n(t) = w(t)$, the signal is affected only by background AWG noise with variance σ^2, whereas in a bad state, i.e., $b(t) = 1 \ \rightarrow \ n(t) = w(t) + k(t)$, it is also affected by IN. The model parameters need to be extracted from measurements for the considered propagation environment [7].

In [8] authors raised a question *What is the right model for wireless channel interference, from a networking standpoint?*, i.e., what is the impact of the interference model chosen for description of various types of networks (ad hoc, sensor, mesh, ...). Three interference models were investigated, namely (i) additive interference model, (ii) capture threshold model, (iii) protocol model. In model (i), a wireless signal is decoded by treating the sum of all the other on-going signal transmissions and environmental disturbances, as noise. The decoding is probabilistic and is successful provided BER overcomes certain acceptable value (SINR has to exceed an appropriate threshold). Denoting the transmit power used by the transmitter of link l as P_l, the SINR perceived by the receiver of link m, SINR_m, is given by:

$$\mathrm{SINR}_m = \frac{G_{m_o,m_d} P_m}{P_{\mathcal{N}} + \sum_{l \in \mathcal{L} \backslash \{m\}} G_{l_o,m_d} P_l}, \tag{1}$$

where $G_{X,Y}$ denotes the channel gain from the point X to the point Y, l_o denotes the transmitter and l_d the receiver of link l, and $P_{\mathcal{N}}$ denotes the thermal noise power in the frequency band of operation. The sum in the denominator is taken over all links $l \in \mathcal{L} \backslash \{m\}$ where $\mathcal{L}$ denotes the set of concurrently active links. The data-rate of link m, c_m, depends on the modulation and coding scheme used at the physical layer on link m. A packet reception at the data-rate c_m is successful, provided that throughout the duration of the packet transmission $\mathrm{SINR_m} \geq \beta_{\mathrm{m}}$, where β_m is an SINR threshold corresponding to an acceptable BER, depending on the modulation and coding scheme used by link m. The Capture threshold model (ii), also used in the ns2 simulator [9], makes use of three thresholds: receive threshold `RxThresh`,

capture threshold `CpThresh` (both analogous to the SINR threshold β described above) and carrier-sensing threshold `CsThresh`. A packet reception on a link m at the data-rate c_m is successful, provided that during the packet transmission $P_m G_{m_o,m_d} \geq \texttt{RxThresh}_m$ and $P_m G_{m_o,m_d} / P_l G_{l_o,m_d} \geq \texttt{CpThresh}_m$ $\forall l \in \mathcal{L} \backslash \{m\}$. Hence, the interference is accounted for only one interferer at a time. For carrier-sensing, a node at Y will sense the channel busy if $P_l G_{l_o,Y} \geq \texttt{CsThresh}_m$ for some active l, where `CsThresh` is the carrier-sensing threshold analogous to β_{cs} from model (i), i.e.

$$\sum_{l \in \mathcal{L}} P_l G_{l_o,Y} + P_{\mathcal{N}} \geq \beta_{cs}. \tag{2}$$

According to the protocol model (iii) in [8], a packet transmission on link m is successful, provided that for each link $l \in \mathcal{L} \backslash \{m\}$ we have $|l_o - m_d| \geq (1 + \Delta) |m_o - m_d|$ and $|m_o - m_d| \leq R_c$, where Δ is a positive parameter and R_c stands for communication range. The capture threshold model is equivalent to the protocol model under isotropic path loss. The interference range model (iv) assumes fixed ranges for communication and interference. According to the this model, a packet reception on link m is successful, provided that for each link $l \in \mathcal{L} \backslash \{m\}$ we have $|l_o - m_d| \geq R_I$ and $|m_o - m_d| \leq R_c$, where R_I stands for interference range and R_c stands for communication range. The interference range model requires the interferer-receiver separation to be greater than a fixed quantity, the interference range, rather than proportional to the transmitter-receiver separation as in the protocol model (iii). Further details and three case studies are given in [8]. An important conclusion is that different physical layer models can lead to different results and applicability of particular interference models.

It is also essential to study the statistics of SINR. The direct approach to compute the average of SINR and its higher moments requires knowledge of the probability density function of SINR, which is difficult to obtain in general. Authors of [1] discuss the problem of finding $\mathbb{E}[\text{SINR}^n]$ is related to the problem of finding the n^{th} negative moments of positive random variables. New exact expressions for the first and second-order averages $\mathbb{E}[\text{SINR}^n]$, $n = 1, 2, \ldots$, and $\mathbb{E}[\text{SINR}_1 \text{SINR}_2]$, where SINR_1 and SINR_2 denote the SINR at two different instances (different sampling times, frequencies or geometrical locations). The practical calculation uses tables of Mellin transforms and special functions. SINR analysis of correlated exponential and log-normal random variables is discussed, together with numerical examples for a CDMA cell with imperfect power control. It was shown that SINR decreases when the useful signal becomes correlated with the interference signals. On the other hand, when the useful signal becomes independent of the interference signals then a positive correlation among the interference signals results in an increase in the average SINR. That is, correlated interfering signals are more harmful than the corresponding independent signals.

Early SINR approaches can be found in CDMA networks [10], where interference and power control in fading radio channels was studied. In CDMA networks each user can transmit a message simultaneously over the same radio bandwidth using specific pseudo-random code sequences. Systems which rely on improved performance from coding and interleaving, however, may require more rapidly acting power control (it is assumed that the power control is performed at a higher rate than the rate of multipath fading). Two different feedback power control algorithms were taken into account: fixed step power control and average power control. A simulation was performed with many concurrent users in a square area and the average interference was observed. The model of power control is idealised, i.e., it assumes a perfect absolute power measurement at each base station. For this reason the work was extended in [11], where a power control based on SINR was studied. In general, if the short-term variation of SINR is negligible compared to that of the desired signal, there is no performance distinction between power control using absolute signal measurement and that based on the measurement of SINR. When a system with SINR-based power control approaches its capacity limit, all the users must increase their power to minimize the effect of thermal noise. A power change of any user will affect the interference seen by all other users and create some degree of positive feedback to the individual control processes. The performance of a system using SIR-based power control depends greatly on how the power control threshold of each user is set [11].

Stuedi and Alonso [12] studied capacity of wireless multi-hop networks under various interferences and radio propagation models, including the physical interference model and log-normal shadowing radio propagation (signal strength perceived by a certain node not only depends on the distance between transmitter and receiver, but also includes some random factor). The protocol and the physical inter-

ference model were taken into account. In the protocol model, a transmission from a node u is said to be received successfully by another node v if no node w closer to the destination node is transmitting simultaneously. However, in practice, nodes outside the interference range of a receiver might still cause enough cumulated interference to prevent the receiver from decoding a message from a given sender. This behavior is captured by the physical model, where a communication between nodes u and v is successful if the SINR at v (the receiver) is above a certain threshold. Network capacity analysis was explained using a conflict graph (transmissions that cannot be scheduled simultaneously). Authors conclude that there was a significant performance gap between capacity under the physical interference model and capacity under the most commonly used protocol model. It was shown that taking into account log-normal radio propagation creates more interference but also decreases the total amount of transmission to be scheduled.

An efficient inter-site interference model for 4G wireless networks was introduced in [13]. The conventional manner in simulating complex topologies (e.g., 4G wireless networks) is to implement a two-tier network (i.e. 19 sites, 57 hexagonal sectors) and subsequently evaluate the performance of user equipment UE from the inner tier. Alternatively, only one tier is simulated and the central site (i.e. the three central sectors) is accounted for the evaluation of performance while the 6 remaining sites are again discarded. The work was motivated by the need for an evaluation platform that provides proper inter-site interference across the region of interest without wasting computational power. The method [13] allows for use with limited resources in contrast to traditional wrap-around techniques with toroid-shaped topologies. The duplication of virtual eNBs is involved at indicated positions exclusively during the interference calculation. All features of the eNBs are replicated, avoiding additional overheads on the complexity of the system.

Conventional investigations on the capacity of a secondary link in spectrum sharing environments have assumed that a secondary user knows perfect channel information between the secondary transmitter and primary receiver. However, this channel information may be outdated at the secondary user because of the time-varying properties or feedback latency from the primary user. If the secondary user allocates transmission power using this outdated channel information, the interference power to the primary receiver will not satisfy the predetermined interference constraint. Kim *et al.* [14] investigated the performance of secondary user while considering interference power constraints, the outdated CSI, and the interference from the primary transmitter (PTx). In the spectrum sharing model (primary and secondary receiver and transmitter, referred here to as PRx, PTx, SRx and STx, respectively), secondary user can share the primary user's spectrum, as long as the amount of interference inflicted on the PRx is within a predetermined constraint. Since the secondary user shares the spectrum of the primary user only within the predetermined interference power constraint, the PRx receives interference from the STx within the predetermined interference power. Furthermore, the SRx also receives interference from the PTx. A point-to-point flat Rayleigh fading channel is assumed, h_0, h_1, h_2 denote instantaneous complex Gaussian channel values from the STx to the PRx and from the STx to the SRx, and from the PTx to the SRx, respectively. The instantaneous channel gains are then denoted by $g_0 = |h_0|^2$, $g_1 = |h_1|^2$, $g_2 = |h_2|^2$, respectively. The CSI on h_0 provided to the STx is outdated due to the time-varying nature of the wireless link. This imperfect CSI can be described by a correlation model, in which

$$h_0 = \rho\widehat{h}_0 + \widetilde{h}_0\sqrt{1-\rho^2}, \tag{3}$$

where $\widehat{h}_0$ is the outdated channel information which the secondary user knows, and $\widetilde{h}_0$ is a complex Gaussian random variable with zero mean and unit variance, and is uncorrelated with $\widehat{h}_0$. The correlation coefficient ρ is a constant which determines the average quality of the channel estimate over all channel states of h_0. The ergodic capacity of the secondary user under the average received-power constraint is derived solving rather complicated optimization problems, for details see [14]. Only lower and upper bound of the capacity could be derived in a closed-form. The SINR in this case can be written as

$$\mathrm{SINR} = \frac{g_1 P\left(\rho, \widehat{g}_0, g_1\right)}{N_0 B + g_2 P_{\mathrm{PTx}}}, \tag{4}$$

where P_{PTx} is the transmission power at the PTx. Both analytical and simulated results demonstrated that the ergodic capacity of the secondary user under the average received-power constraint is more robust to the outdated channel environment than the peak received-power constraint.

In contemporary 4G LTE networks, SINR is not defined by 3GPP but is currently been defined as a "Channel Quality Indicator" (CQI), which reports to the network [15]. Also, there are detailed simulation studies of the loss of throughput for various victim-aggressor scenarios [16]. Reference Signal Received Power (RSRP) and Reference Signal Received Quality (RSRQ) also would apply [17], which would be determined by a measured SINR. Traditionally, a target link quality is characterized by a tolerable bit error rate that, in turn, maps to a required SINR [18]. The SINR is an efficient criterion for several radio resource management algorithms such as power control, data rate adaptation algorithms and cell handoff. There exist various techniques for SINR estimation for various scenarios and wireless standards (e.g., cellular TDMA [19], CDMA [20], fast rate adaptation systems such as 3G HSDPA [18], MIMO systems [21], WLAN [22]). Classical methods of communication theory are generally insufficient to analyze these new types of networks for the following reasons [23]:

- The performance-limiting metric is the SINR rather than the SNR.
- The interference is a function of the network geometry on which the path loss and the fading characteristics are dependent upon.
- The amount of uncertainty present in large wireless networks far exceeds the one present in point-to-point systems: it is impossible for each node to know or predict the locations and channels of all but perhaps a few other nodes.

Two main tools have recently proved most helpful in circumventing the above difficulties: stochastic geometry and random geometric graphs (see the [23] and references therein, or the newer work [24]). Stochastic geometry allows to study the average behavior over many spatial realizations of a network whose nodes are placed according to some probability distribution. Random geometric graphs capture the distance-dependence and randomness in the connectivity of the nodes. Perhaps the largest impact has been in the area of ad hoc networks, which are fully distributed and in which all participating nodes - both transmitters and receivers - are randomly located. In such networks, it is impossible even with unlimited overhead to control the SINRs of all users, due to the coupling of interference: if one user raises its power, it causes an interference increase to all other communicating pairs. In this case, characterizing the (stochastic) geometry of the network is of utmost importance since it is the first-order determinant of the SINR.

In 4G LTE networks [25], the following metrics are used: RSRP is the most basic of the physical layer measurements. It is an expression of the linear average of the downlink Reference Signals, in watts, across the channel bandwidth. Providing the UE with knowledge of absolute RSRP, is essential, since it provides information about the strength of cells from which path loss can be calculated, and afterwards used in optimization algorithms. However, the measure of RSRP give no indication of the signal quality. The RSSI represents the entire recieved power, which is radiated onto the UE, including wanted power from the serving cell, as well as all other co-channel power and noise. Given RSRP and RSSI, the RSRQ is an important measure, since it is defined as a ratio between RSRP and RSSI. A mathematical expression of RSRQ can be seen in equation

$$\mathrm{RSRQ} = \#\mathrm{RB}_{dB} + \frac{\mathrm{RSRP}}{\mathrm{RSSI}}, \tag{5}$$

where #RB (resource block) is the physical amount of bandwidth which can be scheduled on the eNB and are allocated to the UE. The Ressource Block is the smallest unit, that can be scheduled. It physically occupies 180 kHz in frequency, and 0.5 ms in time. Thus for a channel bandwidth of 10 MHz (including guardspaces, etc.), a maximum of 50 RBs can be alotted. For the full channel bandwidth of 20 MHz, there are 100 RBs available.

In IEEE 802.11 wireless LAN it has been shown that simple theoretical models to predict the impact of interference in wireless networks, e.g. using simple path loss models, have very limited accuracy in realistic and relatively complex deployment scenarios (many environment and hardware-specific factors must be considered and empirically testing every group of links is not practical: a network with n nodes can have $O(n^2)$ links, and even if we consider only pairwise interference, we may have to potentially test $O(n^4)$ pairs, see, e.g., [26]). Consequently, there has been a trend towards measurement-based approaches. A comparison of three different measurement-based models is performed in [22], namely the RSS profile

method, the SNR profile method and the SINR profile method. The authors conclude that across all evaluations, the results show that an interference model that uses an SINR profile consistently performs the best in predicting the PDR performance of a wireless link.

1. RSS profile method
   In this model, measurements of pairs {PDR, RSS} between pairs of nodes are performed by having each node taking turns to broadcast packets, and every other node measuring the packet PDR and corresponding RSS. The PDR value is defined as the ratio of the number of packets successfully received to the number of packets sent, while the RSS values are retrieved from the captured packet traces at the receiving node [22]. At every node, the set of these tuples is plotted to obtain an "RSS profile" for that node, which can be interpreted as the probability of successful packet reception as a function of the measured RSS. The authors conclude that the RSS profile is dependent on the environment in which it is constructed.

2. SNR profile method
   In addition to measurements of the pairs {PDR, RSS} between pairs of nodes, measurements of the noise floor at each node are also taken [27]. The SNR value is then computed as the ratio of the RSS value to the NF value. At every node, the set of the pairs {PDR, SNR} is then plotted to obtain an "SNR profile" for that node. In order to use the SNR profile to predict the PDR performance of a wireless link in the presence of interferers, one needs to first know the RSS of the individual interferers. This can be easily obtained from the initial measurements of RSS between pairs of nodes, during the SNR profile construction phase. The RSS values (in mW) corresponding to the concurrent sender and interferers are then used as input into the equation [22]

$$\text{SINR} = \frac{\overline{R}_{sr}}{\sum_i \overline{R}_{t_i r} + NF}, \tag{6}$$

   where $\overline{R}_{sr}$ is the mean RSS of sender s as measured at receiver r during the initial SNR profile construction phase, $\overline{R}_{t_i r}$ is the mean RSS of interferer t_i as measured at receiver r during the initial SNR profile construction phase and NF is the mean noise floor at receiver r. The computed SINR value is then used to lookup the SNR profile to determine the corresponding PDR value.

3. SINR profile method
   In [28], a slightly different measurement approach is proposed to construct SINR profile. First, measurements of RSS between pairs of nodes are performed, similar to [27]. Next, concurrent transmissions from a sender and an interferer are carried out, and the receiver records the number of packets it receives correctly from the sender. This is then used to compute the PDR of the sender-receiver link, in the presence of the interferer. The corresponding SINR value is computed in (6), by using the values of the sender's and the interferer's RSS values, and the noise floor NF at the receiver. Different pairs of sender, interferer nodes are used to generate many pairs of PDR, SINR, which are then used to construct the SINR profile.

2.1.3 Pre-5G wireless channel interference

The ns2 network simulator [9] was further improved and now version ns3 [29] also contains a mmWave module and simple channel and interference models for future 5G systems [30]. As for interference, a model suitable for LTE networks was adopted (Mutual Information Based Effective SINR (MIESM)). The receiver computes the error probability for each transport block (TB) and determines whether the packet can be decoded or not. After the reception of the data packets, the physical (PHY) layer calculates the SINR of the received signal taking into account the MIMO beamforming gains. The physical layer at the user device maps the calculated SINR into a CQI, which is fed-back to the base station for the resource allocation. The TB can be composed of multiple codeblocks (CB) and its size depends on the channel capacity. The block error probability (BLER) of each CB depends on its size and associated modulation and coding schemes (MCS):

$$C_{\text{BLER},i}\left(\gamma_i\right) = \frac{1}{2}\left[1 - \text{erf}\left(\frac{\gamma_i - b_{\text{C}_{\text{SIZE}},\text{MCS}}}{\sqrt{2}c_{\text{C}_{\text{SIZE}},\text{MCS}}}\right)\right], \tag{7}$$

where γ_i is the mean mutual information per coded bit of the codeblock i, $b_{\mathrm{C_{SIZE}},\mathrm{MCS}}$ and $c_{\mathrm{C_{SIZE}},\mathrm{MCS}}$ corresponds to the mean and standard deviation of the Gaussian cumulative distribution, respectively. The TB block error rate can then be computed as:

$$T_{\mathrm{BLER}} = 1 - \prod_{i=1}^{C} \left(1 - C_{\mathrm{BLER},i}\left(\gamma_i\right)\right). \tag{8}$$

In case of failure, the PHY layer does not forward the incoming packet to the upper layers and, at the same time, triggers a retransmission process (this can be a TCP retransmission, or an hybrid automatic repeat request (HARQ)). The interference computation is still relevant in future 5G networks working in millimetre wave bands, despite the directionality of multiantenna propagation. In fact, there might be some special spatial cases where interference is non-negligible [30]. An interference computation scheme was proposed which takes into account the beamforming directions associated with each link. The beamforming gain from transmitter i to receiver j is given as

$$G(t,f)_{ij} = \left|\mathbf{w}^{*}_{rx_{ij}}\mathbf{H}(t,f)_{ij}\mathbf{w}_{tx_{ij}}\right|^2, \tag{9}$$

where $\mathbf{H}(t,f)_{ij}$ is the channel matrix of ij^{th} link, $\mathbf{w}_{tx_{ij}}$ is the beamforming vector of transmitter i when transmitting to receiver j and $\mathbf{w}_{rx_{ij}}$ the beamforming vector of receiver j, when receiving from transmitter i. For instance, if we want to calculate interference between user equipment UE_1 and base station BS_1 (with presence of interfering base station BS_2 and user equipment UE_2), one can write

$$\mathrm{SINR}_{11} = \frac{\frac{P_{Tx,11}}{PL_{11}}G_{11}}{\frac{P_{Tx,22}}{PL_{21}}G_{21} + BW \cdot N_0}, \tag{10}$$

where $P_{Tx,11}$ is the transmit power of BS_1, PL_{11} is the pathloss between BS_1 and UE_1 and $BW \cdot N_0$ is the thermal noise.

Venugopal *et al.* [31, 32] characterized the performance of millimeter-wave wearable communication networks, such as IEEE 802.11ad (WiGig), Wireless HD and device-to-device operating modes proposed for millimetre wave-based 5G cellular systems. A limited region and a finite number of interferers at fixed locations was considered and an approach for calculating coverage and rate in such a network was developed. In crowded environments such as train cars or airline cabins, human bodies are a main and significant source of blockage of millimetre wave frequencies. Nakagami (Gamma) fading was used in simulations. From the locations of the transmitters and blockages, a CCDF of the SINR was found. The network topology considered in [31] is a finite-sized 2D network region $\mathcal{A}$ with a reference transmitter-receiver pair and K potentially interfering transmitters. The transmitters and their locations are denoted by X_i, $i = 0, 1, \ldots, K$, where X_0 is the reference transmitter location. The reference receiver is located at the origin and represents X_i as a complex number $X_i = R_i e^{j\phi_i}$, where $R_i = |X_i|$ is the distance to the i^{th} transmitter and $\phi_i = \angle X_i$ is the angle to X_i from the reference receiver. The CCDF is calculated as follows: a discrete random variable I_i for $i = \{1, \ldots, K\}$ is defined, representing the relative power radiated by X_i in the direction of the reference receiver. With probability $(1 - p_t)$, X_i does not transmit and hence $I_i = 0$. Otherwise, the relative power will depend on whether or not the random orientation of X_i's antenna is such that the reference receiver is within the main-lobe. An uniform orientation of X_i's antenna is assumed and thus the probability that the reference receiver is within its main-lobe is $\frac{\theta_t}{2\pi}$. It follows that

$$I_i = \begin{cases} 0 & \text{with probability } (1 - p_t) \\ G_t & \text{with probability } p_t\left(\frac{\theta_t}{2\pi}\right) \\ g_t & \text{with probability } p_t\left(1 - \frac{\theta_t}{2\pi}\right) \end{cases}, \tag{11}$$

where G_t is the transmitter main-lobe, g_t is the receiver main-lobe, θ_t is the beamwidth of the antenna main-lobe at the transmitter. The normalized power gain from X_i is then defined as

$$\Omega_i = \begin{cases} \frac{P_i}{P_0}G_r R_i^{-\alpha i} & \text{if } -\frac{\theta_r}{2} \leq \phi_i - \phi_0 \leq \frac{\theta_r}{2} \\ \frac{P_i}{P_0}g_r R_i^{-\alpha i} & \text{otherwise} \end{cases}. \tag{12}$$

The SINR is then calculated as

$$\mathrm{SINR} = \frac{h_0 \Omega_0}{\sigma^2 + \sum_{i=1}^{K} I_i h_i \Omega_i}, \tag{13}$$

where $\Omega_0 = G_r R_0^{-\alpha_0}$ is the normalized power gain from the reference transmitter, as the reference transmitter is always assumed to be within the main beam of the reference receiver. Authors of [31, 32] observed a significant improvement in coverage probability with larger antenna arrays, and concluded that having more transmit antennas is more advantageous than having more receive antennas.

Numerous studies are referenced in [33] on wireless interference models, capacity analysis of multi-antenna cellular networks and cooperative transmission in wireless communications. As authors of [33] claim, however, in all the referenced capacity studies, only simple scenarios, such as a single cell with finite interfering transmitters, were considered and the underlying channel models were limited to simple flat Rayleigh fading channels. They derived the exact downlink average capacity of multi-cell MIMO cellular network with co-channel interference, and the analytical closed-form normalized downlink average capacity for cell-edge users in a multi-cell MISO cooperative cellular network with co-channel interference was derived and analyzed numerically. Their analysis indicates that the cooperative transmission can efficiently enhance the capacity performance, especially in scenarios with high densities of interfering BSs.

A mobility-aware uplink interference model for 5G heterogeneous networks (a mix of macro cells and small cells) is presented in [34]. Based on the Lévy flight moving model, an interference model is proposed to characterize the uplink interference from macro cell users to small cell users. The total uplink interference is characterized by its moment generating function, for both closed subscriber group and open subscriber group femto cells. In addition, the proposed interference model is a function of basic step length, which is a key velocity parameter of Lévy flights.

Traditional network models such as the rectangular or hexagonal grid are becoming increasingly obsolete. This is mainly caused by the fact that these approaches do not allow to account for a massive irregular deployment of base stations. A new circular interference model that aggregates given interferer topologies to power profiles along circles is introduced in [35]. A mapping procedure that preserves the aggregate interference statistics at arbitrary user locations within the associated cell with a certain desired accuracy is presented. At the same time, the method identifies the number of nodes in a given interferer topology that principally determine the shape of the interference distribution. The approach allows decomposing the distribution of the aggregate interference into the contributions of the individual interferers. This enabled to accurately model the interference statistics of fully random, heterogeneous topologies with 10 000 and more base stations by some ten nodes in the entire associated cell. Moreover, the proposed method enables accurate prediction of the corresponding SIR and rate statistics.

A statistical inter-cell interference model for downlink cellular OFDMA networks under log-normal shadowing and multipath Rayleigh fading was introduced in [36]. Most of the previous results on the performance evaluation of cellular OFDMA networks have been based on the Gaussian approximation of the inter-cell interference. Accurately taking into account the statistics of the interference could drastically improve the decoded performance. The network model considered in the paper is a homogeneous, synchronous, downlink cellular OFDMA network, one QAM modulated symbol per mobile is transmitted in one of the available subcarriers in each OFDM symbol where the subcarriers are chosen randomly from the available subcarriers. Taking FFT of the discrete-time complex baseband equivalent received samples for a duration of an OFDM symbol, one can derive the final decision variable for each subcarrier, which represents the effects of ICI and the AWGN. Then the PDF of the decision variable is derived and the validity is verified using a Monte Carlo simulation. The maximum-likelihood decoder based on the derived PDF significantly outperforms the traditional decoder optimized for the AWGN channel.

Improving the network throughput (how fast the network may deliver data) and improving the network lifetime (how long the network may last) are two important design objectives for multihop wireless networks, which appear to be in conflict with each other and a trade-off must be identified. Authors of [37] consider wireless networks that are operated by scheduling link transmissions to be conflict-free, as opposed to a random access MAC protocol (supported, e.g., by IEEE 802.16 and LTE cellular networks). A realistic interference model is used based on the SINR for modeling the conflicts to avoid when scheduling the wireless links. It is assumed that the interference to a certain link is the cumulative

interference from the multiple links that are activated during the same period of time. Three optimization problems are formulated: (i) to maximize the network lifetime while achieving the max-min network throughput; (ii) to maximize the network throughput while achieving a pre-specified network lifetime; (iii) to maximize the network lifetime while achieving a fraction of the max-min throughput. Flow routes and link schedules are jointly selected to achieve the desired objective. The channel gain is modelled as isotropic path-loss. The feasibility of a wireless link is based on whether a BER less than a tolerable maximum can be achieved on the link. This BER requirement translates into a minimum SINR requirement corresponding to a SINR threshold $\beta(z)$, depending on modulation scheme z.

2.2 Prior art protected by patent

2.2.1 Jeske, 2003, US20030016740

Jeske [38] proposes SINR estimation for BPSK, but not limited to BPSK. The method claims to improve the square mean error of the conventional SMV estimator by scaling and translation. Noise and interference are modelled together as additive white Gaussian noise (AWGN). The channel attenuation and phase shift is assumed to be fixed over a timeslot. The square mean error of the estimator is further improved by forming a composite SINR using both the pilot and data symbols: a pilot symbol based SINR estimate and a data symbol based SINR estimate are weighted and combined to generate a composite SINR estimate having a reduced mean square error as compared to either of the individual estimators. This is because the pilot symbols have the advantage of being known at the receiver but are relatively fewer in number. Data symbols are more plentiful than pilot symbols but they are unknown at the receiver. The combination of both thus improves the accuracy.

2.2.2 Olszewski, 2004, US20030223354

Olszewski [39] proposes Fast-Fourier transform (FFT)-based SINR measurements methods for wireless communications systems which employ OFDM for multicarrier data transmission. Given a known transmitted time-domain OFDM frame preamble, and the corresponding channel and interference-plus-noise (IPN) corrupted received time-domain frame preamble, the method first computes the power spectral densities of the received signal of interest and of a received unwanted interference-plus-noise signal. The FFT-computed power spectral densities are then used to compute average received signal and received IPN power measurements for specified individual or groupings of OFDM subchannel signals. The power measurements are then frame-averaged using a recursive exponential smoothing method. The frame-averaged signal and IPN power measurements are then used to form quantized measurements of SINR for the specified OFDM subchannel signals of the received frame.

2.2.3 Des Noes, 2010, Patent US7751468

Des Noes [40] proposes SINR estimation for OFDM-CDMA. The invention takes account of the effect of synchronization errors, independent of the value of the codes. The synchronization errors considered includes the offset between carrier frequencies of the transmitter and the receiver and the offset between the transmitter and receiver sampling clocks. The SINR can be estimated for an OFDM-CDMA system using a 2-dimensional spread in the time and frequency domains, or for aa OFDM-CDMA system using a 2-dimensional spread with a channel varying in time. If the codes are orthogonal, the SINR may be estimated taking account of the orthogonality of the codes.

2.2.4 Kangas, 2011, Patent US7986919

Kangas [41] proposes a recursive method of calculating an inverse impairments matrix used to generate an SINR estimate, which in turn is used to generate a CQI estimate. The recursive inverse impairments matrix calculation avoids the need to perform a computationally intensive matrix inversion, allowing for faster CQI estimate generation and consuming less power. Channel conditions from each transmit antenna to each receive antenna are estimated and a matrix of estimated channel noise covariance is generated. An initial inverse impairment matrix for a given pilot position is calculated based on the channel conditions and the channel noise covariance. An inverse impairment matrix is recursively calculating for the pilot

position by recursively summing the noise and inter-stream interference, beginning with the initial inverse impairment matrix. An SINR is then calculated based on the recursively calculated inverse impairment matrix.

2.2.5 Grant, 2011, Patent US20110026566

Grant [42] also discussed the problem with employing the conventional CPICH based SINR estimation approach for MIMO. First is the additional interference created by the reuse of spreading codes on the HS-DSCH (data) channel when in dual-stream mode. Such so-called code-reuse interference does not exist on the CPICH (pilot) channel since the pilots transmitted on each antenna are orthogonal. Hence use of the conventional CPICH-based SINR estimation approach yields an over-estimate of data channel quality leading to excessively high block error rates and thus significantly reduced throughput. In addition, precoding is used on the HS-DSCH whereas no precoding is used on the CPICH. Precoding also affects SINR, hence SINR values calculated using the conventional CPICH-based SINR estimation approach yields an even more inaccurate representation of the data channel quality since precoding is not employed on the pilot channel upon which SINR is solely derived. To address these issues, a method is proposed which enables pilot-based SINR estimation for MIMO system through a combination of parametric and non-parametric approaches.

2.2.6 Semenov, 2012, Patent US20120201285A1

Semenov [43] proposes an apparatus and method for SINR estimation for HSDPA MIMO receiver. The SINR evaluation is based on both the pre-coded data stream and pilot signal. The received data stream is first processed through by an equalizer with a set of equalizer filter coefficients. The inter-stream interference is evaluated based on the post equaliser channel coefficients and the set of weighting coefficients for the pre-coded stream.

2.2.7 Sesia, 2012, Patent US20120310573

Sesia [44] proposes a method based on the estimation done only on a selected number of samples. In particular, only the most reliable samples are selected for the SINR estimation. It claims that through identification of a group suppresses the problem of miss identification of a single sample and by withdraw of samples subjected to intersymbol interference enables a reduction of the contribution of interference in noise calculation which overestimates the SINR calculation.

2.2.8 Zhang, 2012, Patent EP2 398 269A1

Zhang [45] commented that the conventional methods measure the SINR based on SRS (Sounding Reference signal) or DMRS (Demodulation Reference Signal). The problem with these method is that the SRS or DMRS sent by the UE are distributed randomly relative to the channel resource of the UE to be estimated, that is, the relative position of the channel resource occupied by the SRS or DMRS sent by the UE and the channel resource of the UE to be estimated is not fixed. As a result, obtaining the SINR by only using the SRS or DMRS, the accuracy of the SINR estimates for different channel resources to be estimated is not stable. The method proposed is to evaluate the channel correlation. The more accurate SINR is calculated based on SRS-based SINR, DMRS-based SINR and channel correlation. The channel correlation between the channel resource occupied by the last SRS sent by the UE and the channel resource is determined by:

- time offset sensitivity of a wireless channel
- time offset between the channel resource occupied by SRS and user data
- frequency offset sensitivity of a wireless channel
- frequency offset between the channel resource occupied by SRS and user data

2.2.9 Jia, 2013, Patent US8416881

Jia [46] proposes a method for determining an effective SINR associated with transmission of modulation symbols with different modulation schemes (e.g., QPSK, 16QAM, 64QAM) in OFDM systems. Each subcarrier of a channel may have a different SINR. The method proposed in the patent maps the instantaneous SINR of multiple subcarriers into an effective channel SINR (given particular channel state). The transmissions can be separate transmissions that are combined together, such as in A-HARQ retransmissions or FEC blocks, or it can be a single transmission of a data block using different modulation schemes, such as spatial multiplexing in a MIMO transmission.

2.2.10 Semenov, 2013, Patent US008553803B2

In another patent [47] Semenov pointed out that the application of MIMO systems to WCDMA HSDPA systems is problematic with regards to calculating or estimating the SINR. In particular it is not practical to use the same methods used in conventional HSDPA approaches to estimate the SINR for D-TxAA HSDPA modes of operation. In conventional WCDMA implementations the SINR is calculated using pilot symbols with a known pattern and signal strength and measuring the difference between the received and expected symbols. In a MIMO implementation data is typically split into at least two streams and the data symbols are pre-coded with the help of pre-coding weights whilst the pilot symbols are transmitted on a separate channel, the Common Pilot Channel (CPICH), without pre-coding. As the CPICH pilot symbols are not pre-coded, it is not possible to use the conventional SINR estimation methods. An apparatus is thus proposed which generates fake pre-pilot signals by applying the beamforming weighting coefficients so as to enable the decoder to use this knowledge to calculate the SINR for MIMO.

2.2.11 Bontu, 2014, Patent US20140233408

Bontu [48] proposes a method and system for formulating an SINR metric for cells using only the existing RSRP and RSRQ measurements. In certain technologies, such as OFDM, a communication channel is implemented through multiple sub-carriers. Each sub-carrier may have different modulation order, and different SINR at a particular instant in time.

2.2.12 Mizrahi, 2014, Patent US008630335

Mizrahi [49] recognised the limitation of conventional SINR measurement using a Mean Square Error (MSE) estimator. An MSE estimator takes a difference between a received signal and symbols decoded from the received signal, and calculates the mean square error. But such an estimator is only efficient when transmitted symbols are discrete and the receiver is phase locked. In the situation of low SINR, and the receiver is not phase locked, the MSE method cannot estimate SNR accurately, because the decisions are not reliable. Therefore, the author proposed non-data aided (NDA) estimator for low SINR measurement. An NDA estimator is an estimator that estimates SINR without knowledge of the actual transmitted data.

2.3 MIMO Systems

MIMO systems involve the transmission of several modes at the same frequency, whereby there is self a interference between the modes that are not fully orthogonal in practice, but where two or more users are operating in the same cell, each transmission mode is vulnerable to interference from the transmission modes of other users. The same vulnerability is also at risk where a mobile device is on a cell edge and may receive interference from a base station of a neighboring cell transmitting the modes. In [50], simultaneous real time 4x4 MIMO measurements from three base stations to the same mobile were analysed at 5 GHz for the cell edge scenario simultaneously in real time. Such measurements could then determine the real time scale of interference from neighbouring cells due to lack of orthogonality between their respective eigenvectors. Signal to interference ratio was determined by analysis of the singular values and singular vectors computed by the singular value decomposition (SVD) from the wanted channel in the cell within which the mobile was positioned and the interfering channels from neighboring cells. Other analysis was carried out in [51] by analyzing the interference between two mobile users from the same base station.

Computation of the SIR is first defined by taking the power of the first eigenmode, equivalent to the first eigenvalue (or square of the singular value of a wanted time variant channel in base station A, $\mathbf{H}_{\mathrm{A}}(t)$ defined as follows:

$$s_{1\mathrm{A}}^2(t) = \left|\mathbf{u}_{1\mathrm{A}}^H(t)\,\mathbf{H}_{\mathrm{A}}(t)\,\mathbf{v}_{1\mathrm{A}}(t)\right|^2, \tag{14}$$

where the singular vectors of the first eigenmode channel with the highest diversity order, $\mathrm{u}_{1\mathrm{A}}$ and $\mathrm{v}_{1\mathrm{A}}$ are determined by SVD. The term ^{H} is the Hermitian transpose. At a cell edge to cell B, there will be an interfering channel in real time, $\mathbf{H}_{\mathrm{A}}(t)$ which will also have corresponding singular vectors, $\mathrm{u}_{1\mathrm{B}}$ and $\mathrm{v}_{1\mathrm{B}}$ for a mobile in use in that cell. The base station will be transmitting modes with singular vector $\mathrm{v}_{1\mathrm{B}}$ but the mobile in cell A will receive the modes from cell B non orthogonally and without diversity when it is set with vector $\mathrm{u}_{1\mathrm{A}}$ yielding an interference term to define the SIR as follows:

$$\mathrm{SIR} = \frac{s_{1\mathrm{A}}^2(t)}{\left|\mathbf{u}_{1\mathrm{A}}^H(t)\,\mathbf{H}_{\mathrm{B}}(t)\,\mathbf{v}_{1\mathrm{B}}(t)\right|^2}. \tag{15}$$

This therefore shows a ratio of the transmitted power in cell A of the highest eigenmode with diversity to the interference from cell B on that one eigenmode. In MIMO there are at least two eigenmodes and so it is possible that the SIR can be defined in a similar manner for any eigenmode n as follows:

$$\mathrm{SIR} = \frac{s_{n\mathrm{A}}^2(t)}{\left|\mathbf{u}_{n\mathrm{A}}^H(t)\,\mathbf{H}_{\mathrm{B}}(t)\,\mathbf{v}_{n\mathrm{B}}(t)\right|^2}. \tag{16}$$

Similarly the SIR can be analysed this way for comparing interference between two mobiles A and B. These definitions of SIR will give a theoretical limit of SIR available in a fully orthogonal MIMO transmission. Other beamforming methods will not yield a fully orthogonal transmission of modes which will have a self interference and thus the SIR will be lower in practice than the SIR evaluated by SVD and therefore the SIR achieved is dependent on the beamforming scheme used.

Zhang [52] analysed the SINR impairment due to frequency offset and channel estimation errors in MIMO-OFDM. The channel is assumed to be frequency-selective Rayleigh fading. It shows that the interference can be decomposed into two independent components: inter-carrier interference and interference contributed by other transmit antennas. Based on the analysis of the demodulated signal and interference, SINR for each receive antenna is derived. The SINR for MIMO OFDM systems with equal gain combining (EGC) and maximal ratio combining (MRC) are also derived.

The evaluation of SINR for MIMO system can be different when different detector is employed. When the linear minimum mean-squared error (LMMSE) detector is used, the SINR can be explicitly computed for each spatial stream using channel estimates. However, this is not the case for the optimal maximum likelihood (MLD) detector which is gaining growing interest in research and practice. Abe [53] studies the computation of SINR per spatial stream when MLD is employed in MIMO-OFDM spatial multiplexing systems.

The MIMO signal processing usually employs complicated signal processing schemes, e.g. eigenmode beamforming. Parallel transmission as a means of simplifying these schemes was studied by several authors. In parallel transmission, however, the channel capacity is greatly degraded due to the interference from adjacent antenna elements. Authors of [54] proposed a simple method for canceling interference by using antenna directivities. Following system model is considered: two antenna arrays are facing each other, the transmitter has N_t antennas and the receiver has N_r antennas. It is considered that the propagation environment is static and free space. All antennas have vertical polarization for simplicity. The received signal $\mathbf{y}(t) \in \mathbb{C}^{N_r \times 1}$ can be expressed as $\mathbf{y}(t) = \mathbf{H}_0\mathbf{s}(t) + \mathbf{n}(t)$, where $\mathbf{H}_0 \in \mathbb{C}^{N_r \times N_t}$ is a channel matrix and $\mathbf{s}(t) \in \mathbb{C}^{N-T \times 1}$ is a transmit signal vector and $\mathbf{n}(t) \in \mathbb{C}^{N_r \times 1}$ is a noise vector with all components having identical variance. For short-range transmission, the environment is static and the channel response depends on the gain and the phase rotation between transmit and receive antennas. Thus, the component of $\mathbf{H}_0$, which is the channel response from the j-th transmit antenna to the i-th receive antenna, is expressed as $h_{i,j} = \frac{\lambda_0}{4\pi d_{i,j}} \exp(-j\alpha_{i,j})$, where λ_0 is the wavelength, $d_{i,j}$ is the distance and $\alpha_{i,j}$ is the phase rotation between the j-th transmit and the i-th receive antennas, respectively. The

SINR of the parallel transmission is calculated as

$$\mathrm{SINR}_i = \frac{|h_{i,j}|^2 P_\mathrm{s}}{\sum\limits_{j \neq i} |h_{i,j}|^2 P_\mathrm{s} + P_\mathrm{n}}, \tag{17}$$

where P_s is the transmit signal power per stream and P_n is a noise power. From SINR, the channel capacity can be calculated. An optimal spacing of antennas for minimal interference and maximum capacity is calculated in [54].

Different MIMO schemes are affected in different ways in the presence of CCI, and inversely, different MIMO schemes cause different interference. The impact of interfering MIMO schemes on other MIMO schemes is studied in [55].

2.4 Massive MIMO systems

In massive MIMO systems, a common rule-of-thumb is that these systems should have an order of magnitude more antennas M than scheduled users K because the users' channels are likely to be near-orthogonal when $M/K > 10$ [56]. However, it has not been proved that this rule-of-thumb actually maximizes the spectral efficiency. Authors of [57] analyze how the optimal number of scheduled users K depends on M and other system parameters. A cellular network is considered where payload data is transmitted with universal time and frequency reuse. Each cell is assigned an index in the set $\mathcal{L}$. The subset of active UEs changes over time, thus the name UE $k \in \{1, \ldots, K\}$ in cell l in $\mathcal{L}$ is given to different UEs at different times. The geographical position $\mathrm{z}_{lk} \in \mathbb{R}^2$ of UE k in cell l is therefore an ergodic random variable with a cell-specific distribution. Hence, all the channels are static within the frame; $\mathbf{h}_{jlk} \in \mathbb{C}^N$ denotes the channel response between BS j and UE k in cell l in a given frame. The effective SINR for uplink is defined as

$$\mathrm{SINR}_{jk}^{(\mathrm{ul})} = \frac{p_{jk} \left| \mathbb{E}_{\{\mathrm{h}\}} \left\{ \mathbf{g}_{jk}^{\mathrm{H}} \mathbf{h}_{jjk} \right\} \right|^2}{\sum\limits_{l \in \mathcal{L}} \sum\limits_{m=1}^{K} p_{lm} \mathbb{E}_{\{\mathbf{h}\}} \left\{ \left| \mathbf{g}_{jk}^{\mathrm{H}} \mathbf{h}_{jlm} \right|^2 \right\} - p_{jk} \left| \mathbb{E}_{\{\mathbf{h}\}} \left\{ \mathbf{g}_{jk}^{\mathrm{H}} \mathbf{h}_{jjk} \right\} \right|^2 + \sigma^2 \mathbb{E}_{\{\mathbf{h}\}} \left\{ \| \mathbf{g}_{jk} \|^2 \right\}}, \tag{18}$$

where the definition of particular symbols can be found in [57]. A Similar SINR equation is derived for downlink and ergodic achievable spectral efficiencies of an arbitrary UE are calculated for both uplink and downlink. The new spectral efficiency expressions that are independent of the instantaneous UE positions, due to power control and averaging over random UE locations. In fact, the new expressions are the same for the UL and DL, which allows for joint network optimization. Authors provide the reader with full MATLAB code of their approach so that a reproducible research can be conducted (see the references in [57]).

A low-complexity transmission strategy in downlink multi-user MIMO large-scale antenna system was proposed in [58]. The adaptive strategy adjusts the precoding methods, denoted as the transmission mode, to enhance the system sum rate performance. Deterministic sum rate approximations are discussed for the block diagonalization zero-forcing (BDZF), the cooperative zero-forcing (CZF) and the cooperative matched-filter (CMF) modes. First the system model is defined: a downlink system composed of an M-antenna base station and K simultaneously served N-antenna users. The authors assume $M \geq K$, so that user scheduling is not taken into account. Perfect CSI is assumed available at the base station. The base station sends N_k data streams to the k-th user ($1 \leq N_k \leq N$), so that the total number of data streams of the system is $L = \sum_{k=1}^{K} N_k$. The transmitted signal $\mathbf{x} \in \mathbb{C}^{M \times 1}$ is defined as

$$\mathbf{x} = \mathbf{W}\mathbf{s} = \sum_{k=1}^{K} \mathbf{W}_k \mathbf{s}_k, \tag{19}$$

where $\mathbf{W} = [\mathbf{W}_1, \ldots, \mathbf{W}_k] \in \mathbb{C}^{M \times L}$ is the total precoding matrix at the base station, and $\mathbf{s} = \left[\mathbf{s}_1^H, \ldots, \mathbf{s}_K^H\right]^H \in \mathbb{C}^{L \times 1}$ is the information-bearing vector from the base station to all the K users. $\mathbf{W}_k \in \mathbb{C}^{M \times N_k}$ and $\mathbf{s}_k \in \mathbb{C}^{N_k \times 1}$ denotes the precoding matrix and the data vector for the k^{th} user, respectively. N_k antennas

are pre-selected at the k^{th} user to receive signals and the $N_k \times 1$ received signal vector is $\mathbf{y}_k = \mathbf{H}_k\mathbf{x} + \mathbf{n}_k$, where $\mathbf{H}_k \in \mathbb{C}^{N_k \times M}$ with independent circularly-symmetric complex Gaussian distribution $\mathcal{CN}(0,1)$ entries in the channel matrix from the base station to the k^{th} user, $\mathbf{n}_k \in \mathbb{C}^{N_k \times 1}$ with $\mathcal{CN}\left(0, \sigma_n^2\right)$ entries is the additive white Gaussian noise at the k^{th} user.

1. In the BDZF mode, BD technique is utilized to precancel inter-user interference followed by ZF precoders to remove the inter-stream interference of each user. Hence, $\mathbf{W}_k$ is defined as a cascade of two matrices, i.e., $\mathbf{W}_k = \alpha_k \mathbf{B}_k \mathbf{D}_k$, where α_k is the power control parameter. The SINR of data stream (k,i), i.e., the i^{th} received data stream of the k^{th} user is given by

$$\text{SINR}_{k,i}^{\text{BDZF}} = \frac{PN_k}{\sigma_n^2 L \text{tr}\left(\overline{\mathbf{H}}_k \overline{\mathbf{H}}_k^H\right)^{-1}}, \tag{20}$$

   where P is the total available transmit power.

2. For CZF, the MU-MIMO system is treated as an equivalent single-user MIMO system. The equivalent channel $\mathbf{H} \in \mathbb{C}^{L \times M}$ from the base station to all the K users is $\mathbf{H} = \left[\mathbf{H}_1^H, \mathbf{H}_2^H, \ldots, \mathbf{H}_K^H\right]^H$. The CZF precoding matrix is $\mathbf{W}_{\text{CZF}} = \beta \mathbf{H}^H \left(\mathbf{H}\mathbf{H}^H\right)^{-1}$, where β is a parameter normalizing the transmit power. The SINR of data steam (k,i) is then

$$\text{SINR}_{k,i}^{\text{CZF}} = \frac{P}{\sigma_n^2 \text{tr}(\mathbf{H}\mathbf{H}^H)^{-1}}. \tag{21}$$

3. For CMF, the MU-MIMO system is also treated as a SU-MIMO system. MF instead of ZF precoding is utilized. The CMF precoding matrix is $\mathbf{W}_{\text{CMF}} = \gamma \mathbf{H}^H$, where γ is a parameter to normalize the transmit power. For details on the definition of α, β, γ refer to [58]. The corresponding SINR is

$$\text{SINR}_{k,i}^{\text{CMF}} = \frac{\gamma^2 \|\mathbf{h}_{k,i}\|^4}{\sigma_n^2 + \gamma^2 \mathbf{h}_{k,i} \left(\sum_{(l,m)\neq(k,i)} \mathbf{h}_{l,m}^H \mathbf{h}_{l,m}\right) \mathbf{h}_{k,i}^H}. \tag{22}$$

The main objective of precoding in a Massive MIMO system is to improve the gain of the large-scale antenna array and mitigate the impact of pilot contamination. This problem was solved in several papers. Authors of [59] investigated an algorithm on Max-SINR criterion and improved it for Massive MIMO. There exist several precoding methods with their upper-bound performance (discussed in references within [59]). The Max-SINR criterion had been an important criterion in the research of interference cancelling and used in Multi-user MIMO precoding and cooperative transmission of Multi-cells. The interference part of SINR counts the impact of the channel estimation error and the character of MIMO channel. The objective function assures to maximize the utilization rate of the transmission power under the condition that SINR is not lower than the desired threshold. The Lagrangian function was optimized by Karush-Kuhn-Tucker (KKT) conditions and the optimal downlink precoding matrix was obtained. The system model is as follows: there are I cells and each cell serves K UEs in Massive MIMO system. Base station of each cell is equipped with N_t antennas and per user equipment configures a single antenna. $\mathbf{f}_{jk}^j$ is the channel matrix from the base station of cell j to UE k of cell j, $\mathbf{a}_{jk}$ is the precoding matrix. The downlink SINR of user k in cell j is then expressed as following (further details and derivations can be found in [59]):

$$\text{SINR}_{jk} = \frac{\left|\mathbf{f}_{jk}^j \mathbf{a}_{jk}\right|^2}{1 + \sum\limits_{\substack{i=1 \\ i\neq j}}^{I} \sum\limits_{k=1}^{K} \left|\mathbf{f}_{jk}^i \mathbf{a}_{ik}\right|^2}. \tag{23}$$

According to the channel reciprocity, the downlink channel is equal to the uplink channel and we can write $\mathbf{f}_{jk}^j = \left(\mathbf{H}_{jk}^j\right)^T$. A real channel information is defined $\mathbf{H}_{jk}^j = \sqrt{\beta_{jk}^j}\mathbf{h}_{jk}^j$. It cannot be acquired in solving the downlink precoding matrix and is usually replaced by the estimated channel information

$\widehat{\mathbf{H}}_{jk}^{j}$. To maximize SINR_{jk}, the precoding matrix should not only achieve the maximal gain of desired signals, but also minimize the power of pilot pollution and the interference power. So the SINR in (23) is rewritten as following:

$$\mathrm{SINR}_{jk} = \frac{\left|\sqrt{\beta_{jk}^{j}}\left(\widehat{\mathbf{H}}_{jk}^{j}\right)^{T}\mathbf{a}_{jk}\right|}{1+\left|\sum\limits_{\substack{l=1\\l\neq j}}^{L}\sum\limits_{k=1}^{K}\sqrt{\beta_{lk}^{j}}\left(\mathbf{h}_{lk}^{j}\right)^{T}\mathbf{a}_{jk}\right|^{2}+\sum\limits_{\substack{i=1\\i\neq j}}^{I}\sum\limits_{k=1}^{K}\left|\sqrt{\beta_{jk}^{i}}\left(\mathbf{h}_{jk}^{i}\right)^{T}\mathbf{a}_{ik}\right|^{2}}. \tag{24}$$

Under the condition that SINR_{jk} of user k in cell j is greater than the desired threshold, the objective of downlink Massive MIMO precoding should ensure to maximize the utilization rate of the transmission power and minimize the total power consumption. An objective function is written and the optimal precoding matrix $\mathbf{a}_{jk}$ is found by solving Lagrange equation (see [59] for details). Numerical results proved that Max-SINR precoding algorithm outperform than the traditional Massive MIMO precoding – the matched-filter algorithm.

Similar approach was adopted in [60], where a channel approximation method based on compressive sensing was used to estimate the most dominant singular subspaces of the global multicell MIMO channel matrix. Then, the estimate of the global channel information is used to design an intercell-interference-aware zero-forcing multicell precoding method in the downlink to mitigate not only the intracell interference but also the intercell interference of the channel.

The matched filter (MF) beamforming is attractive technique due to its low complexity of implementation compared to beamforming techniques such as zero-forcing, and minimum mean square error. A specific problem in applying these techniques is how to qualify and quantify the relationship between the transmitted signal, channel noise and interference. In [61] a procedure was presented of deriving an approximate formula for PDF of the SINR at user terminal when multiple antennas and MF beamformer are used at the base station. The solution of this problem is very important, because this PDF is necessary to compute the probability of symbol error and outage performance of massive MIMO.

For further reading on Massive MIMO, there exist a regularly updated Massive MIMO Research Library [62] with references to papers from various areas of Massive MIMO (architecture, capacity, precoding algorithms etc). An introduction to the topic is also contained in dissertation [63].

2.5 Standards activities

The IEEE 802.16 Working Group on Broadband Wireless Access Standards has been maintaining standards for wireless metropolitan area networks, including advanced radio interface, multi-tier networks, enhancements to support machine-to-machine applications and others (for the list of active and draft-stage standards see [64]). Different radio noise measurement methods, sources of noise and requirements for the measurement equipment are discussed in [5]. SINR requirements for testing of LTE and E-UTRA UE radio transmission and reception are discussed in standard [65], the physical layer for 4G LTE networks is described in [66] and the physical channel and modulation formats for the 4G networks are described in standard [67].

There exist several standards discussing the interference management in mobile networks. Standards for 5G systems will build on the knowledge gained in previous standards. As the future networks will bring a radical paradigm change, many new standards are expected. Industry will play the major role in 5G infrastructure with respect to the necessary long-term investment in global standardization. Early consensus among major stakeholders on these systems must be achieved prior to global 5G standardization activities.

3 Key elements of 5G

Key industrial players shard their visions about the future communications, connected society and smart cities, global challenges and key technology drivers and innovations (see, e.g., [68–74]). Global collaboration will be crucial for finding a solution to all the very challenging technical problems.

3.1 Defining characteristics of 5G

There exist several overview papers on the requirements of future 5G systems (general overview [75], challenges for backhaul traffic model [76], the role of small cells, coordinated multipoint, and massive MIMO in 5G [77], regularly updated database of papers on Massive MIMO [62]). 5G will need to be a paradigm shift that includes very high carrier frequencies with massive bandwidths, extreme base station and device densities, and unprecedented numbers of antennas. However, unlike the previous four generations, it will also be highly integrative: tying any new 5G air interface and spectrum together with LTE and WiFi to provide universal high-rate coverage and a seamless user experience. To support this, the core network will also have to reach unprecedented levels of flexibility and intelligence, spectrum regulation will need to be rethought and improved, and energy and cost efficiencies will become even more critical considerations.

Industry initiatives, such as GSMA's December 2014 paper on 'Understanding 5G: Perspectives on future technological advancements in mobile', progressed thinking on 5G. It identified a set of eight core-requirements:

1. 1-10 Gbps connections to end points in the field (i.e. not theoretical maximum)
2. 1 millisecond end-to-end round trip delay (latency)
3. 1000× bandwidth per unit area
4. 10-100× number of connected devices
5. (Perception of) 99.999 % availability
6. (Perception of) 100 % coverage
7. Reduction in network energy usage
8. Up to ten year battery life for low-power, machine-type devices

The UK Spectrum Policy Forum ("UK SPF") [78] vision for 5G [79], developed by the UK SPF 5G working group, was submitted by Ofcom to the relevant preparatory group for The International Telecommunications Union ("ITU"). It is not identical, but along similar lines to these 8 core requirements. NGMN published a paper in February 2015 [68] further exploring the 5G requirements and providing analysis supporting the requirements and challenges to be addressed. The paper is aligned in terms of the scope of this paper. An extract states (page 9 of [68]):

> *In 5G, NGMN anticipates the need for new radio interface(s) driven by use of higher frequencies, specific use cases such as Internet of Things (IoT) or specific capabilities (e.g., lower latency), which goes beyond what 4G and its enhancements can support. However, 5G is not only about the development of a new radio interface. NGMN envisions 5G as an end-to-end system that includes all aspects of the network, with a design that achieves a high level of convergence and leverages today's access mechanisms (and their evolution), including fixed, and also any new ones in the future.*

Achieving the eight requirements above, requires a significant change with respect to networks and services and how industry addresses the challenges they present. Previously, evolution saw access networks evolve in silos (e.g. 2G, 3G, 4G, Wi-Fi, Fixed, Fibre, Cable etc.). In the 5G world all of these have to be working in a converged manner, transparent to the user and leveraging best available assets to achieve the bandwidth, density, capacity, quality of service and latency required. Additionally, existing services which require multi-network hops rely on non-deterministic internet based connectivity and interworking (which 5G has the opportunity to address the requirements across multiple network-boundaries), and optimize and dynamically negotiate the required network connectivity parameters such as QoS, speed and latency, based on the service requirement or context of the 'User' or 'Thing' being connected.

The earlier mobile phone generations (2G-4G) use specifically licensed spectrum. Within the spirit of the 5G concept there is the possibility of supplementing this with the use of unlicensed bands and

duplex transmission. Under these conditions it is likely that different signaling and contention-avoidance strategies will be in play, making interference the main problem as the power levels at which disruption of communication occurs will be different.

Within these eight requirements, the speed of connection and latency are the most likely to be affected by noise and interference issues. There may also be an effect on the power used within the network.

3.2 Overview of expected noise and interference in 5G

Mainly the CCI and ISI are studied in single-carrier systems. In case of the OFDM, also the ICI must be taken into account. The ICI is caused by transmitter and receiver analog processing impairments such as in-phase/quadrature imbalance. Various SINR formulas can be defined, depending on which noise and interference sources are taken into account. For example, approximate SINR analysis for OFDM systems under high mobility is reported in [80]. For multiple-antenna OFDM systems, approximate SINR analysis for MIMO spatial multiplexing, space-time coded OFDM systems, and MIMO beamforming can be found in [81], [82], and [83], respectively.

Advanced interference cancellation (IC) of common and unicast signals includes a combination of linear and nonlinear interference cancellation techniques [84]. Linear IC refers to spatial minimum mean squared error (MMSE) processing, while nonlinear IC involves estimating and reconstructing the interference signal at the victim receiver, and subtracting the reconstructed interference from the received signal, before decoding the desired signal. Nonlinear IC may involve estimating the interference signal at the modulation symbol level (SLIC) or at the codeblock level (CLIC). Error propagation issues associated with SLIC may be overcome by adopting a soft cancellation approach, incorporating the confidence level in estimated interference symbols. CLIC is mostly immune to error propagation effects, but requires that the spectral efficiency targeted by the interfering transmitter be consistent with the interference signal quality ($I/(S + N)$) at the victim receiver. Both approaches require knowledge of various transmission parameters of the interfering signal, such as the modulation order, spatial multiplexing scheme, pilot type (common/dedicated), and traffic-to-pilot ratio. Advanced techniques such as decentralized coordination and interference alignment/neutralization are being actively researched, and may well find application in fifth generation (5G) cellular systems [84].

3.3 5G Signalling Methods

There are several proposals on how to solve interference issues in future 5G networks. Coexistence of cognitive radio (CR) systems with existing licensed systems is discussed in [85]. An interference temperature model is introduced for this purpose to characterize the interference from the CR to the licensed networks. Interference cancellation techniques should also be applied to mitigate the interference at CR receivers. The interference management in 4G LTE is mostly a network based operation and transparent to receivers. Authors of [86] propose that advanced interference management (AIM) techniques should be the key driver of 5G initiation, which consist of UE-side as well as network-side interference management techniques. Various practical challenges are discussed, such as realistic interference conditions, receiver architecture and CSI reporting. With conventional receivers, a single CSI report per UE was assumed, since the receiver characteristic is not dependent on the interference signal rate. However, with advanced receivers, a single CSI report is often too short for describing the peculiar relationship between the receiver characteristic and the interference signal rate [86]. To address this problem, a multiple-CSI feedback framework could be adopted, which was already introduced for coordinated multipoint (CoMP) support in LTE Release 11.

3.4 Device to device consideration

Device-to-device (D2D) communication allows nearby devices to establish local links so that traffic flows directly between them instead of through base stations. D2D communication can potentially improve user experience by reducing latency and power consumption, increasing peak data rates, and creating new proximity-based services such as proximate multiplayer gaming. D2D communication leads to dense spectrum reuse. The base station is no longer the traffic bottleneck between the source and destination.

The ad hoc nature of D2D communication results in very irregular interference topology with large signal dynamic range [84].

In [87] a two-tier cellular network is envisaged that involves a macrocell tier (i.e., BS-to-device communications) and a device tier (i.e., device-to-device communications). Device terminal relaying makes it possible for devices in a network to function as transmission relays for each other and realize a massive ad hoc mesh network. In such a two-tier cellular system, security must be maintained for privacy. To ensure minimal impact on the performance of existing macrocell BSs, the two-tier network needs to be designed with smart interference management strategies and appropriate resource allocation schemes. In case of no BS is used (i.e., the source and destination devices have direct communication with each other without any operator control), there is no centralized entity to supervise the resource allocation between devices. Operating in the same licensed band, devices will inevitably impact macrocell users. The smart interference management include approaches such as resource pooling, non-cooperative game or bargaining game, admission control and power allocation, cluster partitioning, and relay selection (for details, see the references in [87]).

3.5 Millimetre-wave frequencies

In the previous mobile communication systems all mobile cellular systems are deployed in sub-3 GHz spectrum. Even including Wi-Fi systems the frequencies are still below 6 GHz. One possible area of 5G study is to explore higher carrier frequency, such as millimetre-wave bands (30 to 300 GHz) where there is currently less pressure on the spectrum use [88]. Two salient features of the millimetre-wave bands are large amounts of bandwidth, enabling very high in coverage throughput, and very small wavelengths enabling a large number of tiny antennas in a given device area. The main challenges for millimetre-waveband communications include large path loss (especially with Non-Line-of-Sight, NLoS, propagation), signal blocking/absorption by various objects in the environment, and low transmit (Tx) power capability of current millimetre-wave-band amplifiers. Highly directional beams improve the link budget and enable very dense spatial reuse through spatial/angular isolation. This massive spatial orthogonalisation leads to a very different cellular architecture where the millimetre-wave base stations can be very densely deployed with significantly overlapping coverage but no strong inter-cell interference.

4 SINR Workshop

A SINR Workshop was held on 9th October 2015 at the University of Surrey. The aim of the workshop was to consult directly with industry and members of standards bodies to identify clear requirements for a definition of SINR as well as traceable methods to characterize such metrics. A presentation with an overview of the EURAMET Metrology for 5G Communications (Met5G, see the webpage [89]) project will be delivered from which a facilitated discussion will take place to achieve this aim. Such outcomes from the workshop will provide valuable guidance on the direction of the Met5G project. Notes from the workshop together with the full transcript of meeting questions are summarized in report [90].

To keep the scope of the discussion within sensible bounds the number of "questions" was limited:

1. Modelling of interference in device testing or system evaluation, Gaussian white noise or other model?
2. Use of the channel quality indicator (CQI) in 5G. Device requirements in capturing signal to interference and noise ratio.
3. Scenarios to characterize interference on wireless devices. Impact of full duplex.
4. Does the interference need to be represented in terms or power and angle?
5. Do we need some indexing to categorize the impact of different noise and interference signals?
6. Choice of signalling or waveform methods to evaluate as SINR candidates for 5G.

A summary of the key responses are that the "interference" contribution is significant and its impact may be disproportional compared with AGWN. This is particularly true for narrow-band and "bursty" signals and their effect on legacy systems. MIMO and other complex antenna systems offer additional degrees of freedom. Consequentially, the definitions may be more complex and possibly an algorithmic approach. An important action to maximise impact is to maintain close liaison with the standards community ETSI mWT, 3GPP etc. to achieve a workable definition that will be adopted.

5 Characterization of interference from NMI perspective

National Measurement Institutes fulfil two main functions: the dissemination and traceability of the SI to fundamental units and underpinning

1. Scientifically rigorous traceable to primary standards - sufficient to be accepted internationally.
2. Practical and useable for industry - any approximations required to do this are defensible. The result must be simple enough to be useful without creating an unacceptable cost burden on industry.
3. Provide a fair basis for international trade - acceptable to the measurement standards bodies.
4. Have understandable confidence intervals.

SNR uses the premise of added Gaussian White-Noise, which is a simple and mathematically defined concept. For SINR we have seen that the impairment may depend on the type of interference, leading to a more complex definition. Also, experimental measures of throughput in a MIMO show that the cut-off from 100 % throughput to 0% throughput. The traceability of SINR measurements will be a challenging task. As was shown in previous sections, the SINR evaluation employs rather complicated mathematical apparatus in order to model the signal to interference and noise ratio. Advanced methods for measurement uncertainty evaluation including Monte Carlo method will be required.

6 Discussion and summary

Previous sections summarized existing approaches of interference evaluation in various systems and indicated challenges in future wireless systems. It is obvious that there exists a need to re-interpret and use SINR for purposes of evaluating system impact at network level. This is particularly apparent in ns2 [9] network models and forthcoming ns3 [29] network models. From the information theory point of view, SINR reduction needs to be also interpreted in terms of capacity change.

The SINR, in its basic form, is expressed as a ratio of signal to the sum of interference signals plus Gaussian white noise. However, dependent on the scenario, it can also bring about a dependency on time, distance, polarisation, angular pattern and frequency. All scenarios are bandwidth dependent. In terms of 5G technology requirements it is necessary to quantify defined scenarios where interference has an impact on quality of service, both to the new 5G system but also in terms of legacy services using neighbouring spectrum bands. This therefore inherently describes suited categories for which there are dependencies on variables applicable in different cases. These have been summarised in Tab. 1.

Currently there exists measurement instrumentation on the market which is able to decode various wireless standards, such as WiMAX, LTE, WiFi and others. However, these instruments do not identify and discard the interfering signals. Traceable measurement of LTE power was discussed in [91] within the EMRP "MORSE" project (for details, see [92]). In the future work, a way to the interference quantifying should be described. One way could be recording of signals and interpreting their signalling (with spectrum knowledge assumption).

Acknowledgement

The results in this paper come from the project MET5G Metrology for 5G communications. This project has received funding from the EMPIR programme co-financed by the Participating States and from the European Union's Horizon 2020 research and innovation programme.

Table 1: Categorisation of SINR definitions, their application, modelling method and dependencies. Note "X" is a definite dependency, "O" is an optional dependency.

Category	**Application**	**Models**	**Dependencies**				
			Time	**Dist**	**Pol**	**Pat**	**Freq**
Mean SINR In Band [1]	Inter-cell interference, cell handover Multi RAT devices with independent radios coexisting Self interference (e.g. Full Duplex)	Gaussian Noise + [Path Loss for far distance or Coupling model for close proximity devices]		X	O	O	
Mean SINR Side Band [2]	Adjacent channel interference Interference to legacy wireless services	Gaussian Noise + [Path Loss for far distance, or Coupling model for close proximity devices] + Signalling and intermodulation distortion model		X	O	O	X
Time Variant SINR In Band [3]	Evaluating the frequency dependency and time variant SINR in band Consideration of impulse noise from narrowband devices, for Internet of Things	Gaussian noise + Path Loss Model + Narrowband or Wideband Fading Model Optional Markov model with carrier wave for Impulse Noise	X	X	O	O	O
Extended Definition of SINR for MIMO [4]	To accommodate the beamforming capability of MIMO, thus fully pattern dependent. To consider interference on the transmission modes for MIMO	All components in Time Variant SINR In Band with the addition of MIMO beamforming and pattern changes	X	X	X	X	O

[1] Distance will inevitably change SINR considering both the distance of the wanted and interfering transmitters from the receiver. The polarisation and pattern effects are optional depending on what path loss model is used and not applicable where coupling of devices in close proximity is concerned. NB: Mean power for the signal and also the interferers may have dependence on the signalling method used.
[2] Additionally to the In Band SINR, it will be necessary to account for the side band noise caused by the signalling method and intermodulation distortion. This will have definite frequency dependence.
[3] The instantaneous SINR of multiple devices nomadically positioned within a cell will have high variation due to scatterers. Polarisation and pattern effects will depend on the model used, whether it is stochastic or deterministic. Frequency dependency is determined by whether the narrowband or wideband case is considered.
[4] The pattern dependency will be essential in this regard due to the impact of applying beamforming on the antenna elements.

References

[1] K. A. Hamdi, "On the statistics of signal-to-interference plus noise ratio in wireless communications," *IEEE Trans. Commun.*, vol. 57, no. 11, pp. 3199–3204, 2009.

[2] L. Zhao and A. M. Haimovich, "Performance of ultra-wideband communications in the presence of interference," *IEEE J. Select. Areas Commun.*, vol. 20, no. 9, pp. 1684–1691, 2002.

[3] T. Jia and D. I. Kim, "Analysis of average signal-to-interference-noise ratio for indoor UWB Rake receiving system," in *IEEE Vehicular Technology Conference (VTC)*, Stockholm, Sweden, May 2005, pp. 1396–1400.

[4] M. Fernandez, I. Landa, A. Arrinda, R. Torre, and M. Velez, "Harmonization of Noise Measurement Methods: Measurements of radio impulsive noise from a specific source," *IEEE Antennas Propagat. Mag.*, vol. 57, no. 5, pp. 64–72, 2015.

[5] "Methods for Measurements of Radio Noise," ITU-R Recommendation Standard," SM.1753-2, 2012. [Online]. Available: http://www.itu.int/rec/R-REC-SM.1753-2-201209-I/

[6] M. Cheffena, "Propagation Channel Characteristics of Industrial Wireless Sensor Networks," *IEEE Antennas Propagat. Mag.*, vol. 58, no. 1, pp. 66–73, 2016.

[7] M. Cheffena, "Industrial wireless sensor networks: Channel modeling and performance evaluation," *EURASIP J. Wireless Communications Networking*, vol. 2012, no. 297, pp. 1–8, 2012.

[8] A. Iyer, C. Rosenberg, and A. Karnik, "What is the right model for wireless channel interference?" *IEEE Trans. Wireless Commun.*, vol. 8, no. 5, pp. 2662–2671, 2009.

[9] "The ns2 network simulator," http://www.isi.edu/nsnam/ns/, Accessed: 2015-11-30.

[10] S. Ariyavisitakul and L. F. Chang, "Signal and interference statistics of a CDMA system with feedback power control," *IEEE Trans. Commun.*, vol. 41, no. 11, pp. 1626–1634, 1993.

[11] S. Ariyavisitakul, "Signal and interference statistics of a CDMA system with feedback power control II," *IEEE Trans. Commun.*, vol. 42, no. 234, pp. 597–605, 1994.

[12] P. Stuedi and G. Alonso, "Log-normal shadowing meets SINR: A numerical study of Capacity in Wireless Networks," in *4^{th} Annual IEEE Communications Society Conference on Sensor, Mesh and Ad Hoc Communications and Networks (SECON)*, San Diego, CA, June 2007, pp. 550–559.

[13] A. Amate, S. Sofianos, M. Milosavljevic, P. Kourtessis, and J. M. Senior, "An efficient inter-site interference model for 4G wireless networks," in *IEEE International Conference on Communications (ICC)*, Budapest, Hungary, June 2013, pp. 5355–5359.

[14] H. Kim, H. Wang, S. Lim, and D. Hong, "On the Impact of Outdated Channel Information on the Capacity of Secondary User in Spectrum Sharing Environments," *IEEE Trans. Wireless Commun.*, vol. 11, no. 1, pp. 284–295, 2012.

[15] "Technical Specification Group Radio Access Network; Evolved Universal Terrestrial Radio Access (E-UTRA); Physical layer procedures," 3GPP TS 36.213, version 12.3.0 Release 12, 2014-09. [Online]. Available: http://www.3gpp.org/dynareport/36213.htm/

[16] "LTE; Evolved Universal Terrestrial Radio Access (E-UTRA); Radio Frequency (RF) system scenarios," 3GPP TR 36.942, version 8.1.0 Release 8, 2009-01. [Online]. Available: http://www.3gpp.org/dynareport/36942.htm/

[17] "Technical Specification Group Radio Access Network; Evolved Universal Terrestrial Radio Access (E-UTRA); Physical layer; Measurements," 3GPP TS 36.214, version 12.0.0 Release 12, 2014-09. [Online]. Available: http://www.3gpp.org/dynareport/36214.htm/

[18] D. R. Jeske and A. Sampath, "Signal-to-Interference-plus-Noise Ratio Estimation for Wireless Communication Systems: Methods and Analysis," *Naval Research Logistics*, vol. 51, no. 5, pp. 720–740, 2004.

[19] M. Turkboylari and G. Stuber, "An efficient algorithm for estimating the signal-to-interference ratio in TDMA cellular systems," *IEEE Trans. Commun.*, vol. 46, no. 6, pp. 728–731, 1998.

[20] D. Ramakrishna, N. B. Mardayam, and R. Yates, "Subspace based SIR estimation for CDMA cellular systems," *IEEE Trans. Veh. Technol.*, vol. 49, no. 5, pp. 1732–1742, 2000.

[21] P. Li, D. Paul, R. Narasimhan, and J. Cioffi, "On the Distribution of SINR for the MMSE MIMO Receiver and Performance Analysis," *IEEE Trans. Inform. Theory*, vol. 52, no. 1, pp. 271–286, 2006.

[22] W. L. Tan, P. Hu, and M. Portmann, "Experimental Evaluation of Measurement-based SINR Interference Models," in *World of Wireless, IEEE International Symposium on Mobile and Multimedia Networks (WoWMoM)*, San Francisco, CA, June 2012, pp. 1–9.

[23] M. Haenggi, J. G. Andrews, F. Baccelli, O. Dousse, and M. Franceschetti, "Stochastic Geometry and Random Graphs for the Analysis and Design of Wireless Networks," *IEEE J. Select. Areas Commun.*, vol. 27, no. 7, pp. 1029–1045, 2009.

[24] M. D. Renzo and P. Guan, "A Mathematical Framework to the Computation of the Error Probability of Downlink MIMO Cellular Networks by Using Stochastic Geometry," *IEEE Trans. Commun.*, vol. 62, no. 8, pp. 2860–2879, 2014.

[25] M. Rumney, Ed., *LTE and the Evolution to 4G Wireless: Design and Measurement Challenges*, 2nd ed. John Wiley & Sons, Inc, 2013.

[26] J. Padhye, S. Agarwal, V. N. Padmanabhan, L. Qiu, A. Rao, and B. Zill, "Estimation of link interference in static multihop wireless networks," in *Proc. ACM IMC*, Berkeley, CA, June 2005, pp. 28–28.

[27] A. Kashyap, S. Ganguly, and S. R. Das, "A measurement-based approach to modeling link capacity in 802.11-based wireless networks," in *Proc. ACM Mobicom*, New York, NY, 2007, pp. 242–253.

[28] R. Maheshwari, S. Jain, and S. R. Das, "A measurement study of interference modeling and scheduling in low-power wireless networks," in *Proc. 6^{th} ACM conference on Embedded network sensor systems (SenSys)*, New York, NY, 2008, pp. 141–154.

[29] "The ns3 network simulator," https://www.nsnam.org/, Accessed: 2016-02-18.

[30] M. Mezzavilla, S. Dutta, M. Zhang, M. R. Akdeniz, and S. Rangan, "5G MmWave Module for the Ns-3 Network Simulator," in *Proc. of the 18^{th} ACM International Conference on Modeling, Analysis and Simulation of Wireless and Mobile Systems*, Cancun, Mexico, Mar. 2015, pp. 1–8.

[31] K. Venugopal, M. C. Valenti, and R. W. Heat, "Interference in finite-sized highly dense millimeter wave networks," in *Information Theory and Applications Workshop (ITA)*, San Diego, CA, Feb. 2015, pp. 175–180.

[32] K. Venugopal, M. C. Valenti, and R. W. H. Jr., "Device-to-Device Millimeter Wave Communications: Interference, Coverage, Rate, and Finite Topologies," *arXiv*, vol. abs/1506.07158, pp. 1–31, 2015. [Online]. Available: http://arxiv.org/abs/1506.07158

[33] X. Ge, K. Huang, C. X. Wang, X. Hong, and X. Yang, "Capacity Analysis of a Multi-Cell Multi-Antenna Cooperative Cellular Network with Co-Channel Interference," *IEEE Trans. Wireless Commun.*, vol. 10, no. 10, pp. 3298–3309, 2011.

[34] Y. Dong, Z. Chen, P. Fan, and K. Letaief, "Mobility-Aware Uplink Interference Model for 5G Heterogeneous Networks," *IEEE Trans. Wireless Commun.*, vol. PP, no. 99, pp. 1536–1276, 2015.

[35] M. Taranetz and M. Rupp, "A Circular Interference Model for Asymmetric Aggregate Interference," *arXiv*, vol. abs/1505.05842, pp. 1–30, 2015. [Online]. Available: http://arxiv.org/abs/1505.05842

[36] C. Seol and K. Cheun, "A statistical inter-cell interference model for downlink cellular OFDMA networks under log-normal shadowing and multipath Rayleigh fading," *IEEE Trans. Commun.*, vol. 57, no. 10, pp. 3069–3077, 2009.

[37] J. Luo, A. Iyer, and C. Rosenberg, "Throughput-Lifetime Trade-Offs in Multihop Wireless Networks under an SINR-Based Interference Model," vol. 10, no. 3, pp. 419–433, 2011.

[38] D. R. Jeske and A. Sampath, "Method of Estimating Signal-to-Interference + Noise Ratio (SINR)," Patent US20 030 016 740, Jan. 23, 2003.

[39] K. J. Olszewski, "SINR Measurement Method for OFDM Communications Systems," Patent US20 030 223 354, Dec. 4, 2004.

[40] M. D. Noes, D. Ktenas, L. Maret, and Y. Nasser, "Estimation of a Signal-to-Interference Plus Noise Ratio at the Output of an OFDM CDMA Receiver," Patent US7 751 468, July 6, 2010.

[41] A. Kangas and M. Ringström, "Simplified Impairments Matrix Calculation for SINR Estimation," Patent US7 986 919, June 26, 2011.

[42] S. Grant, "Pilot-Based SINR Estimator for MIMO Systems," Patent US20 110 026 566, Feb. 3, 2011.

[43] S. Semenov, K. Ostman, A. Malkov, J. Vesma, and R. Paatelma, "Apparatus and Method for SINR Estimation HSDPA MIMO Receiver," Patent US20 120 201 285A1, Aug. 9, 2012.

[44] S. Sesia and A. Ancora, "Method to Estimate a Signal to Interference Plus Noise Ratio Based on Selection of the Samples and Corresponding Processing System," Patent US20 120 310 573A1, Dec. 6, 2012.

[45] Q. Zhang, Y. Li, and W. Liu, "Signal to Interference Plus Noise Ratio (SINR) Estimation Method and Device," Patent EP2 398 269A1, Dec. 21, 2012.

[46] M. Jia, J. Ma, P. Zhu, and W. Tong, "Effective Signal Interference Plus Noise Ratio Estimation for Multi-Order Modulation," Patent US8 416 881, Apr. 9, 2013.

[47] S. Semenov and T. P. Tammilehto, "Estimation of the Signal to Interference and Noise Ratio (SINR) in Multiple Input Multiple Output (MIMO) Systems," Patent US008 553 803B2, Oct. 8, 2013.

[48] C. S. Bontu, Z. Cai, Y. Yu, Y. Song, M. Fong, and R. Hu, "Procedure for Formulating a Signal to Interference Plus Noise Ratio," Patent US20 140 233 408, Aug. 21, 2014.

[49] H. Mizrahi and I. Rosenhouse, "SNR Estimation," Patent US008 630 335, Jan. 14, 2014.

[50] T. W. C. Brown, P. C. F. Eggers, and K. Olesen, "Simultaneous 5 GHz Co-channel MIMO Links at Microcellular Boundaries: Interference or Cooperation?" *IET Microw. Antennas Propag.*, vol. 1, no. 6, pp. 1152–1159, 2007.

[51] T. W. C. Brown, P. C. F. Eggers, and G. F. Pedersen, "Experimental interference assessment between two independent and simultaneous 4x4 MIMO handset user links, operating at 5 GHz," *Electronics Lett.*, vol. 46, no. 4, pp. 309–310, 2010.

[52] W. Zhang, Z. Zhang, and C. Tellambura, "Signal-to-Interference-Plus-Noise Ratio Analysis for MIMO-OFDM with Carrier Frequency Offset and Channel Estimation Errors," in *Wireless Communications and Networking Conference (WCNC)*, Honolulu, HI, Mar. 2007, pp. 927–931.

[53] T. Abe and G. Bauch, "Effective SINR Computation for Maximum Likelihood Detector in MIMO Spatial Multiplexing Systems," in *Global Telecommunications Conference (GLOBECOM)*, Honolulu, HI, Nov. 2009, pp. 1–5.

[54] M. Arai, T. Seki, K. Hiraga, T. Nakagawa, and K. Uehara, "Study on short-range MIMO transmission using interference cancellation by antenna directivities," in *Asia-Pacific Microwave Conference Proceedings (APMC)*, Seoul, South Korea, Nov. 2013, pp. 395–397.

[55] M. I. Rahman, E. de Carvalho, and R. Prasad, "Impact of MIMO Co-Channel Interference," in *18thInternational Symposium on Personal, Indoor and Mobile Radio Communications*, Athens, Greece, Sept. 2007, pp. 1–5.

[56] J. Hoydis, S. ten Brink, and M. Debbah, "Massive MIMO in the UL/DL of cellular networks: How many antennas do we need?" *IEEE J. Select. Areas Commun.*, vol. 31, no. 2, pp. 160–171, 2013.

[57] E. Bjornson, E. G. Larsson, and M. Debbah, "Massive MIMO for Maximal Spectral Efficiency: How Many Users and Pilots Should Be Allocated?" *IEEE Trans. Wireless Commun.*, vol. 15, no. 2, pp. 1293–1308, 2016.

[58] H. Liu, H. Gao, A. Hu, and T. Lv, "Low-complexity transmission mode selection in MU-MIMO systems," in *21st Int. Conf. on Telecommunications (ICT)*, Lisbon, Portugal, May 2014, pp. 6–10.

[59] J. Jing and X. Zheng, "A Downlink Max-SINR Precoding for Massive MIMO System," *International Journal of Future Generation Communication and Networking*, vol. 7, no. 3, pp. 107–116, 2014.

[60] S. L. H. Nguyen and A. Ghrayeb, "Precoding for multicell massive MIMO systems with compressive rank-q channel approximation," in *24thInternational Symposium on Personal, Indoor and Mobile Radio Communications*, London, UK, Sept. 2013, pp. 1227–1232.

[61] S. Feng, G. Chen, W. Mao, S. Berber, and Y. Xiaohu, "Probability density derivation and analysis of SINR in massive MIMO systems with MF beamformer," *arXiv*, vol. abs/1411.0080, pp. 1–12, 2014. [Online]. Available: http://arxiv.org/abs/1411.0080

[62] "Massive MIMO Info Point," https://massivemimo.eu/research-library, Accessed: 2015-11-30.

[63] H. Q. Ngo, "Massive MIMO: Fundamentals and System Designs," Ph.D. dissertation, Linköping University, Sweden, Department of Electrical Engineering, 2013.

[64] "IEEE 802.16 Published Standards and Drafts," http://www.ieee802.org/16/published.html, Accessed: 2016-01-12.

[65] "LTE; Evolved Universal Terrestrial Radio Access (E-UTRA); User Equipment (UE) radio transmission and reception," 3GPP TS 36.101, version 12.5.0 Release 12, 2014-11. [Online]. Available: http://www.3gpp.org/dynareport/36101.htm

[66] "LTE; Evolved Universal Terrestrial Radio Access (E-UTRA); Physical channels and modulation," 3GPP TS 36.211, version 10.0.0 Release 13, 2016-01. [Online]. Available: http://www.3gpp.org/dynareport/36201.htm

[67] "LTE; Evolved Universal Terrestrial Radio Acces (E-UTRA); Physical channels and modulation," 3GPP TS 36.211, version 13.0.0 Release 13, 2016-01. [Online]. Available: http://www.3gpp.org/dynareport/36211.htm

[68] "NGMN 5G White paper," https://www.ngmn.org/uploads/media/NGMN_5G_White_Paper_V1_0.pdf, Accessed: 2015-11-30.

[69] "Looking ahead to 5G," http://networks.nokia.com/file/28771/5g-white-paper, NOKIA, Accessed: 2016-05-31.

[70] "5G Systems," https://www.ericsson.com/res/docs/whitepapers/what-is-a-5g-system.pdf, Ericsson, Accessed: 2016-05-31.

[71] "5G: A Technology Vision," http://www.huawei.com/5gwhitepaper/, Huawei, Accessed: 2016-05-31.

[72] "5G Vision," http://www.samsung.com/global/business-images/insights/2015/Samsung-5G-Vision-0.pdf, Samsung, Accessed: 2016-05-31.

[73] "DOCOMO 5G White paper," https://www.nttdocomo.co.jp/english/binary/pdf/corporate/technology/whitepaper_5g/DOCOMO_5G_White_Paper.pdf, DOCOMO, Accessed: 2016-05-31.

[74] "White Papers on key 5G technologies," http://www.nec.com/en/press/201602/global_20160222_03.html, NEC, Accessed: 2016-05-31.

[75] J. G. Andrews, S. Buzzi, W. Choi, S. V. Hanly, A. Lozano, A. C. K. Soong, and J. C. Zhang, "What Will 5G Be?" *IEEE J. Select. Areas Commun.*, vol. 32, no. 6, pp. 1065–1082, 2014.

[76] X. Ge, H. Cheng, M. Guizani, and T. Han, "5G wireless backhaul networks: challenges and research advances," *IEEE Network*, vol. 28, no. 6, pp. 6–11, 2014.

[77] V. Jungnickel, K. Manolakis, W. Zirwas, B. Panzner, V. Braun, M. Lossow, M. Sternad, R. Apelfröjd, and T. Svensson, "The role of small cells, coordinated multipoint, and massive MIMO in 5G," *IEEE Commun. Mag.*, vol. 528, no. 5, pp. 44–51, 2014.

[78] "UK Spectrum Policy Forum (UK SPF)," https://www.techuk.org/about/uk-spectrum-policy-forum, Accessed: 2015-11-30.

[79] "UK Spectrum Policy Forum, 5G working group vision," https://www.techuk.org/events/meeting/item/1673-uk-5g-vision, Accessed: 2015-11-30.

[80] B. Narasimhan, D. Wang, S. Narayanan, H. Minn, , and N. Al-Dhahir, "Digital compensation of frequency-dependent joint Tx/Rx I/Q imbalance in OFDM systems under high mobility," *IEEE J. Select. Topics Sign. Proces.*, vol. 3, no. 3, pp. 405–417, 2009.

[81] Y. Zou, M. Valkama, and M. Renfors, "Analysis and compensation of transmitter and receiver I/Q imbalances in space-time coded multiantenna OFDM systems," *EURASIP J. Wirel. Comm. and Networking*, vol. 56, no. 391025, pp. 1–16, 2008.

[82] Y. Zou, M. Valkama, and M. Renfors, "Performance analysis of spatial multiplexing MIMO-OFDM systems under frequency-selective I/Q imbalances," in *Int. Wireless Communications and Mobile Computing Conf. (IWCMC09)*, Leipzig, Germany, June 2009, pp. 1381–1386.

[83] O. Ozdemir, R. Hamila, and N. Al-Dhahir, "I/Q imbalance in multiple beamforming OFDM transceivers: SINR analysis and digital baseband compensation," *IEEE Trans. Commun.*, vol. 61, no. 5, pp. 1914–1925, 2013.

[84] N. Bhushan, J. Li, D. Malladi, R. Gilmore, D. Brenner, A. Damnjanovic, R. T. Sukhavasi, C. Patel, and S. Geirhofer, "Network Densification: The Dominant Theme for Wireless Evolution into 5G," *IEEE Commun. Mag.*, vol. 52, no. 2, pp. 82–89, 2014.

[85] C. Wang, F. Haider, X. Gao, X.-H. You, Y. Yang, D. Yuan, H. M. Aggoune, H. Haas, S. Fletcher, and E. Hepsaydir, "Cellular Architecture and Key Technologies for 5G Wireless Communication Networks," *IEEE Commun. Mag.*, vol. 52, no. 2, pp. 122–130, 2014.

[86] W. Nam, D. Bai, J. Lee, and I. Kang, "Advanced Interference Management for 5G Cellular Networks," *IEEE Commun. Mag.*, vol. 52, no. 2, pp. 52–60, 2014.

[87] M. N. Tehrani, M. Uysal, and H. Yanikomeroglu, "Device-to-Device Communication in 5G Cellular Networks: Challenges, Solutions, and Future Directions," *IEEE Commun. Mag.*, vol. 52, no. 5, pp. 86–92, 2014.

[88] T. S. Rappaport, S. Sun, R. Mayzus, H. Zhao, Y. Azar, K. Wang, G. N. Wong, J. K. Schulz, M. Samimi, and F. Gutierrez, "Millimeter Wave Mobile Communications for 5G Cellular: It Will Work!" *IEEE Access*, vol. 1, pp. 335–349, 2013.

[89] "EMPIR 14IND10 'MET5G' Metrology for 5G Communications," http://empir.npl.co.uk/met5g/, Accessed: 2016-02-18.

[90] D. A. Humphreys, T. Brown, and J. R. Kelly, "Notes from the SINR workshop 9$^{\text{th}}$ October 2015 ," Institute for Communication Systems, Univ. of Surrey, UK," MET5G project Activity report, 2015.

[91] S. Dash, F. Pythoud, P. Leuchtmann, and J. Leuthold, "Traceable Power Measurement of LTE Signals," in *17th International Congress of Metrology*, Paris, France, Sept. 2015, p. 12005.

[92] "EMRP IND51 'MORSE' Metrology for optical and RF communication systems," http://projects.npl.co.uk/emrp-ind51-morse/, Accessed: 2016-02-18.